Uniform spin susceptibility and spin-gap phenomenon in the BCS-BEC-crossover regime of an ultracold Fermi gas

Hiroyuki Tajima, Takashi Kashimura, Ryo Hanai, Ryota Watanabe, and Yoji Ohashi
Department of Physics, Keio University, 3-14-1 Hiyoshi, Kohoku-ku, Yokohama 223-8522, Japan
(Received 4 December 2013; published 12 March 2014; publisher error corrected 19 March 2014)

We investigate the uniform spin susceptibility χ_s in the BCS (Bardeen-Cooper-Schrieffer)-BEC (Bose-Einstein condensation) crossover regime of an ultracold Fermi gas. Including pairing fluctuations within the framework of an extended T-matrix approximation, we show that χ_s exhibits nonmonotonic temperature dependence in the normal state. In particular, χ_s is suppressed near the superfluid phase transition temperature T_c due to strong pairing fluctuations. To characterize this anomalous behavior, we introduce the spin-gap temperature T_s as the temperature at which χ_s takes a maximum value. Determining T_s in the whole BCS-BEC crossover region, we identify the spin-gap regime in the phase diagram of a Fermi gas in terms of the temperature and the strength of a pairing interaction. We also clarify how the spin-gap phenomenon is related to the pseudogap phenomenon appearing in the single-particle density of states. Our results indicate that an ultracold Fermi gas in the BCS-BEC crossover region is a very useful system to examine the pseudogap phenomenon and the spin-gap phenomenon in a unified manner.

DOI: 10.1103/PhysRevA.89.033617 PACS number(s): 03.75.Ss, 03.70.+k

I. INTRODUCTION

Recently, the pseudogap phenomenon has attracted much attention in cold Fermi gas physics [1–15]. Although the pseudogap has been also discussed in high-T_c cuprates as a key to clarify the pairing mechanism of this system [16–18], the complexity of this system still prevents us from clarifying the origin of this many-body phenomenon. So far, various possibilities have been discussed, such as superconducting pairing fluctuations [19], antiferromagnetic spin fluctuations [20,21], a hidden order [22,23], a stripe order [24–26], and combined pairing fluctuations with charge order [27]. In addition, anisotropic pseudogap phenomena with the same symmetry as the d-wave superconducting order parameter realized in high-T_c cuprates [28], as well as the importance of quasiparticles in the nodal directions [29], have also recently been discussed experimentally.

On the other hand, an ultracold Fermi gas is much simpler than high-T_c cuprates. In addition, the strength of a pairing interaction in this system can be experimentally tuned by adjusting the threshold energy of a Feshbach resonance [30–34]. This unique property enables us to study the BCS-BEC crossover phenomenon [35–38], where the character of a Fermi superfluid continuously changes from the weak-coupling BCS type to the Bose-Einstein condensation of tightly bound molecules, with increasing the interaction strength [39–44]. Since the intermediate coupling regime is dominated by strong pairing fluctuations, this so-called BCS-BEC crossover region is expected to be useful for the assessment of the preformed-pair scenario, which has been discussed as a possible mechanism of the pseudogap phenomenon in high-T_c cuprates [19].

However, in contrast to our expectation, the pseudogap problem in cold Fermi gas physics is still in debate. While the recent photoemission-type experiments on ^{40}K Fermi gases [9–12] agree with the pseudogap scenario [1–8], a local pressure experiment [13], as well as an experiment on the spin polarization rate [14], on ^{6}Li Fermi gases support the Fermi liquid theory. Since the latter theory is characterized by the existence of stable Fermi quasiparticles with long lifetime τ [45], it is incompatible with a pseudogapped Fermi gas, where the formation of preformed pairs leads to short quasiparticle lifetime τ. Thus, it is a crucial problem whether an ultracold Fermi gas is a Fermi liquid or a pseudogapped Fermi gas.

The pseudogap is a dip structure appearing in the single-particle density of states $\rho(\omega)$ around $\omega = 0$ above the superfluid phase transition temperature T_c [1–8]. Thus, direct observation of $\rho(\omega)$ would be the most effective approach to resolve the pseudogap problem in cold Fermi gas physics. In high-T_c cuprates, such a dip structure has been observed by using scanning tunneling spectroscopy (STS) [16]. However, such a powerful technique does not exist in cold Fermi gas physics, which makes this problem more difficult.

In this paper, as a useful physical quantity to resolve the pseudogap problem in cold Fermi gas physics, we pick up the uniform spin susceptibility χ_s in the BCS-BEC crossover region above T_c. In contrast to the density of states $\rho(\omega)$, χ_s is observable in this gas system [46–48]. In the case of a free Fermi gas, χ_s is known to be proportional to $\rho(\omega = 0)$ far below the Fermi temperature T_F [49]. Thus, when this property still holds in the presence of a pairing interaction, one may detect the pseudogap in (unobservable) $\rho(\omega \simeq 0)$ through the anomaly in χ_s. We note that the suppression of χ_s near T_c is known as the spin-gap phenomenon in the underdoped regime of high-T_c cuprates [50]. Although the origin of the spin gap is still unclear in this system, the importance of a pseudogap for this anomalous magnetic phenomenon has been discussed [51,52]. Since an ultracold Fermi gas in the BCS-BEC crossover region is dominated by strong pairing fluctuations, a study of the spin susceptibility in this system would be helpful to see to what extent the preformed-pair scenario can explain both the pseudogap phenomenon and the spin-gap phenomenon in a unified manner.

In considering the spin-gap phenomenon in an ultracold Fermi gas, one should note that the ordinary strong-coupling theory developed by Nozières and Schmitt-Rink [41,42] as well as the (non-self-consistent) T-matrix approximation (TMA) [44], which have been extensively used to clarify various BCS-BEC crossover physics in this system,

unphysically give negative spin susceptibility in the crossover region [53–55]. However, this serious problem has been recently overcome by including higher-order pairing fluctuations beyond the T-matrix level [55]. In this extended T-matrix approximation (ETMA), the bare Green's functions in the TMA self-energy are partially replaced by the dressed Green's functions so that the spin-vertex correction is consistent with the ETMA self-energy in the sense that the Ward identity can involve the RPA (random phase approximation)-type infinite perturbation series with respect to an effective attractive interaction $-\Gamma_0$ (<0) [55]. The resulting ETMA spin susceptibility $\chi_{\rm s}$ has the form $\chi_{\rm s} \sim \tilde{\chi}_{\rm s}/[1+\Gamma_0\tilde{\chi}_{\rm s}]$ [where $\tilde{\chi}_{\rm s}$ (>0) is the spin susceptibility without vertex correction], which is always positive in the entire BCS-BEC crossover region. In contrast, the RPA series is truncated at $O(\Gamma_0)$ in the TMA, leading to $\chi_{\rm s} \sim \tilde{\chi}_{\rm s}[1-\Gamma_0\tilde{\chi}_{\rm s}]$, which unphysically becomes negative in the strong-coupling regime when $\Gamma_0\tilde{\chi}_{\rm s} > 1$. In addition to this quantitative improvement, it has also been shown [55] that the ETMA spin susceptibility agrees well with the recent experiment on a ^{6}Li Fermi gas [46], as well as the theoretical result in the self-consistent T-matrix approximation [56]. Although the ETMA result disagrees with the experiment done by Sommer and co-workers [47], it has been pointed out that this experiment corresponds to the case with a repulsive interaction [57,58].

In this paper, we employ the ETMA to calculate the temperature dependence of $\chi_{\rm s}$ over the entire BCS-BEC crossover region. Introducing the spin-gap temperature $T_{\rm s}$ as the temperature below which $\chi_{\rm s}$ is anomalously suppressed, we determine the spin-gap regime in the phase diagram of an ultracold Fermi gas in terms of the temperature and the strength of a pairing interaction. We also deal with the single-particle density of states $\rho(\omega)$ within the same theoretical framework, to clarify how the spin-gap phenomenon is related to the pseudogap phenomenon.

This paper is organized as follows. In Sec. II, we explain our formulation. Although the ETMA has been explained in Ref. [55], we present the outline of this strong-coupling formalism so that our paper can be self-contained. In Sec. III, we show our results on the spin susceptibility to determine the spin-gap temperature $T_{\rm s}$ in the BCS-BEC crossover region. We also discuss how the spin-gap phenomenon is related to the pseudogap phenomenon there. In Sec. IV, we separately consider the spin-gap phenomenon in the BEC region. Throughout this paper, we set $\hbar = k_{\rm B} = 1$, and the system volume V is taken to be unity, for simplicity.

II. FORMULATION

We consider a three-dimensional uniform two-component Fermi gas, described by the BCS Hamiltonian

$$H = \sum_{\boldsymbol{p},\sigma}(\varepsilon_{\boldsymbol{p}} - \mu_\sigma)c^\dagger_{\boldsymbol{p},\sigma}c_{\boldsymbol{p},\sigma} - U\sum_{\boldsymbol{p},\boldsymbol{p}',\boldsymbol{q}} c^\dagger_{\boldsymbol{p}+\boldsymbol{q}/2,\uparrow}c^\dagger_{-\boldsymbol{p}+\boldsymbol{q}/2,\downarrow}c_{-\boldsymbol{p}'+\boldsymbol{q}/2,\downarrow}c_{\boldsymbol{p}'+\boldsymbol{q}/2,\uparrow}. \quad (1)$$

Here, $c_{\boldsymbol{p},\sigma}$ is the annihilation operator of a Fermi atom with the kinetic energy $\varepsilon_{\boldsymbol{p}} = p^2/2m$ (where m is an atomic mass) and pseudospin $\sigma = \uparrow,\downarrow$ describing two atomic hyperfine states. μ_σ is the Fermi chemical potential in the σ component. Although we mainly deal with an unpolarized Fermi gas in this paper, the spin-dependent chemical potential is necessary in calculating the spin susceptibility. $-U$ is an assumed tunable pairing interaction. As usual, we measure the interaction strength in terms of the s-wave scattering length $a_{\rm s}$ [42], which is related to the bare interaction $-U$ as

$$\frac{m}{4\pi a_{\rm s}} = -\frac{1}{U} + \sum_{\boldsymbol{p}}^{\omega_{\rm c}}\frac{1}{2\epsilon_{\boldsymbol{p}}}, \quad (2)$$

where $\omega_{\rm c}$ is a cutoff energy [59].

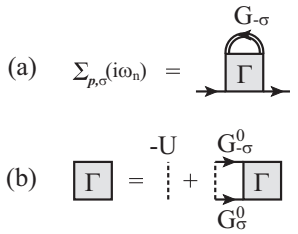

FIG. 1. (a) Self-energy $\Sigma_{\boldsymbol{p},\sigma}(i\omega_n)$ in the extended T-matrix approximation (ETMA). The double solid line and the single solid line are the dressed Green's function $G_{\boldsymbol{p},\sigma}(i\omega_n)$ in Eq. (3) and the bare Green's function $G^0_{\boldsymbol{p},\sigma}(i\omega_n)$ in Eq. (4), respectively. (b) Particle-particle scattering matrix $\Gamma_{\boldsymbol{q}}(i\nu_n)$. The dashed line represents the pairing interaction $-U$.

The ETMA is characterized by the self-energy $\Sigma_{\boldsymbol{p},\sigma}(i\omega_n)$, which is diagrammatically given in Fig. 1 [55]. In this figure, the double solid line describes the dressed single-particle thermal Green's function, given by

$$G_{\boldsymbol{p},\sigma}(i\omega_n) = \frac{1}{\left[G^0_{\boldsymbol{p},\sigma}(i\omega_n)\right]^{-1} - \Sigma_{\boldsymbol{p},\sigma}(i\omega_n)}, \quad (3)$$

where

$$G^0_{\boldsymbol{p},\sigma}(i\omega_n) = \frac{1}{i\omega_n - \varepsilon_{\boldsymbol{p}} + \mu_\sigma} \quad (4)$$

is the Green's function for a free Fermi gas (which is described as the single solid line in Fig. 1). In Eqs. (3) and (4), ω_n is the fermion Matsubara frequency. Summing up the ETMA diagrams in Fig. 1, we obtain

$$\Sigma_{\boldsymbol{p},\sigma}(i\omega_n) = T\sum_{\boldsymbol{q},i\nu_n}\Gamma_{\boldsymbol{q}}(i\nu_n)G_{\boldsymbol{q}-\boldsymbol{p},-\sigma}(i\nu_n - i\omega_n). \quad (5)$$

Here, ν_n is the boson Matsubara frequency. The particle-particle scattering matrix $\Gamma_{\boldsymbol{q}}(i\nu_n)$ in Eq. (5) has the form

$$\Gamma_{\boldsymbol{q}}(i\nu_n) = \frac{-U}{1 - U\Pi_{\boldsymbol{q}}(i\nu_n)}, \quad (6)$$

where

$$\Pi_{\boldsymbol{q}}(i\nu_n) = T\sum_{\boldsymbol{p},i\nu_n} G^0_{\boldsymbol{p}+\boldsymbol{q}/2,\uparrow}(i\nu_n + i\omega_n)G^0_{-\boldsymbol{p}+\boldsymbol{q}/2,\downarrow}(-i\omega_n) = \sum_{\boldsymbol{p}}\frac{1 - f(\epsilon_{\boldsymbol{p}+\boldsymbol{q}/2} - \mu_\uparrow) - f(\epsilon_{-\boldsymbol{p}+\boldsymbol{q}/2} - \mu_\downarrow)}{\epsilon_{\boldsymbol{p}+\boldsymbol{q}/2} + \epsilon_{-\boldsymbol{p}+\boldsymbol{q}/2} - \mu_\uparrow - \mu_\downarrow - i\nu_n} \quad (7)$$

is the lowest-order pair-correlation function, describing fluctuations in the Cooper channel.

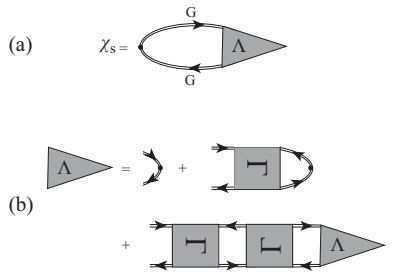

FIG. 2. (a) Feynman diagram describing spin susceptibility χ_s. The dressed Green's function G involves the self-energy correction. The triangle (Λ) is the spin-vertex correction. The solid circle describes the bare spin vertex. (b) The spin-vertex correction Λ consistent with the ETMA self-energy in Fig. 1(a). The particle-particle scattering matrix Γ is diagrammatically given in Fig. 1(b).

Within the framework of the ETMA, the uniform spin susceptibility χ_s can be conveniently calculated from

$$\chi_s = \lim_{h\to 0} \frac{\Delta N}{h} \equiv \lim_{h\to 0} \frac{N_\uparrow - N_\downarrow}{h}, \tag{8}$$

where $h = \mu_\uparrow - \mu_\downarrow$ is a fictitious magnetic field. In this paper, we numerically evaluate Eq. (8) by taking a small but finite value, $h/\varepsilon_F = O(10^{-2})$ [60] (where ε_F is the Fermi energy). The number N_σ of Fermi atoms in the σ component is given by

$$N_\sigma = T \sum_{\boldsymbol{p}, i\omega_n} G_{\boldsymbol{p},\sigma}(i\omega_n). \tag{9}$$

The advantage of using Eq. (8) is that the vertex correction, which is consistent with the ETMA self-energy in Eq. (5), is automatically taken into account. Indeed, by substituting Eq. (9) into Eq. (8), we obtain

$$\chi_s = -T \sum_{\boldsymbol{p}, i\omega_n} [G_{\boldsymbol{p}}(i\omega_n)]^2 \Lambda_{\boldsymbol{p}}(i\omega_n), \tag{10}$$

which is diagrammatically described as Fig. 2(a). In Eq. (10), we have suppressed the spin index σ because we are considering the unpolarized limit ($\mu_\uparrow = \mu_\downarrow = \mu$). We always use this simplified notation in this paper when we deal with this limiting case. In Eq. (10), $\Lambda_{\boldsymbol{p}}(i\omega_n)$ is the spin-vertex correction involving effects of pairing fluctuations, given by

$$\Lambda_{\boldsymbol{p}}(i\omega_n) = 1 - \sum_\sigma \sigma \left. \frac{\partial \Sigma_{\boldsymbol{p},\sigma}(i\omega_n)}{\partial h} \right|_{h\to 0}. \tag{11}$$

Equation (11) is just the Ward identity for the spin-vertex correction [61], which is a required condition for any consistent theory [62]. When we start from Eq. (10) in calculating the spin susceptibility, we need to explicitly evaluate the spin-vertex correction $\Lambda_{\boldsymbol{p}}(i\omega_n)$ involving the derivative of the ETMA self-energy [see Eq. (11)], which is diagrammatically given by Fig. 2(b). In this paper, however, we numerically calculate Eq. (8) so that we can avoid this complicated procedure, and the calculated spin susceptibility satisfies the required Ward identity within the numerical accuracy.

In this paper, we also consider the single-particle density of states $\rho(\omega)$ in the unpolarized case to examine the relation between the spin-gap phenomenon and the pseudogap phenomenon. This quantity is calculated from the analytic continued Green's function as

$$\rho(\omega) = -\frac{1}{\pi} \sum_{\boldsymbol{p}} \mathrm{Im}[G_{\boldsymbol{p}}(i\omega_n \to \omega + i\delta)], \tag{12}$$

where δ is an infinitesimally small positive number.

The superfluid instability is determined from the Thouless criterion, $[\Gamma_{\boldsymbol{q}=0}(i\nu_n = 0)]^{-1} = 0$ [63], which gives

$$1 = \frac{U}{2} \sum_{\boldsymbol{p}} \frac{\tanh \frac{\varepsilon_{\boldsymbol{p}} - \mu}{2T_c}}{\varepsilon_{\boldsymbol{p}} - \mu}. \tag{13}$$

We numerically solve the T_c equation (13), together with the number equation (9), under the condition $N_\uparrow = N_\downarrow = N/2$ (where N is the total number of Fermi atoms). We self-consistently determine T_c and μ for a given interaction strength.

Before ending this section, we briefly note that the self-energy in the ordinary (non-self-consistent) TMA is given by replacing the dressed Green's function G in Eq. (5) with the bare one G^0. To see the difference between the two approximations in calculating the spin susceptibility in a simple manner, it is convenient to approximate the particle-particle scattering matrix Γ in Fig. 2(b) to a constant value ($\equiv -\Gamma_0$). As mentioned in Sec. I, the ETMA spin susceptibility is then described by the RPA-type infinite series as $\chi_s \simeq \tilde{\chi}_s/[1 + \Gamma_0 \tilde{\chi}_s]$. On the other hand, this series is truncated at $O(\Gamma_0)$ in the TMA case as $\chi_s \simeq \tilde{\chi}_s^0[1 - \Gamma_0 \tilde{\chi}_s]$ (where $\tilde{\chi}_s$ is the spin susceptibility without vertex correction). As a result, although the ETMA correctly gives positive χ_s in the whole BCS-BEC crossover region [55], the TMA spin susceptibility unphysically becomes negative in the interesting BCS-BEC crossover region when $\Gamma_0 \tilde{\chi}_s > 1$. For more details, we refer to Ref. [55].

III. SPIN-GAP PHENOMENON AND RELATION TO PSEUDOGAP PHENOMENON IN AN ULTRACOLD FERMI GAS

Figure 3 shows the uniform spin susceptibility $\chi_s(T)$ in a unitary Fermi gas above T_c [$(k_F a_s)^{-1} = 0$, where k_F is

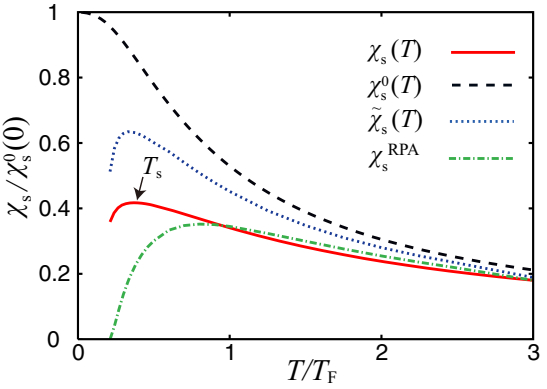

FIG. 3. (Color online) Calculated ETMA uniform spin susceptibility $\chi_s(T)$ in a unitary Fermi gas ($T_c = 0.21T_F$) as a function of temperature. $\chi_s^0(T)$ is the spin susceptibility in the case of a free Fermi gas and T_F is the Fermi temperature. $\tilde{\chi}_s(T)$ is given in the second line in Eq. (15). $\chi_s^{RPA}(T)$ is given in Eq. (19). The arrow shows the spin-gap temperature T_s.

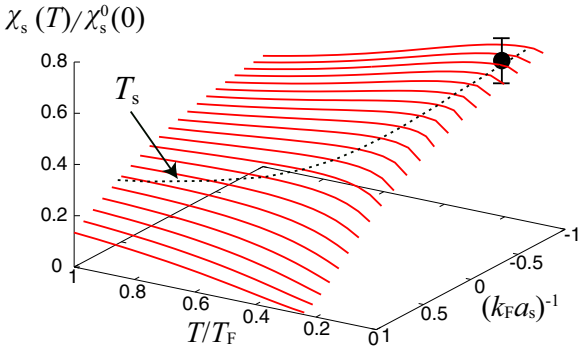

FIG. 4. (Color online) Calculated spin susceptibility χ_s in the BCS-BEC crossover region above T_c (solid line). The dashed line shows the peak position of χ_s, which gives the spin-gap temperature T_s. The filled circle with the error bar is the observed spin susceptibility in a ^{6}Li Fermi gas at $(k_Fa_s)^{-1} \simeq -0.8$ [46] (where k_F is the Fermi momentum).

the Fermi momentum]. In this figure, one sees that $\chi_s(T)$ exhibits nonmonotonic temperature dependence. While the temperature dependence of $\chi_s(T \geqslant 0.37T_F)$ is qualitatively the same as the noninteracting case $[\chi_s^0(T)]$, $\chi_s(T)$ anomalously decreases with decreasing the temperature when $T_c \leqslant T \leqslant 0.37T_F$. Since the latter phenomenon never occurs in the noninteracting case, it is considered to originate from strong pairing fluctuations near T_c. We briefly note that this low-temperature behavior of χ_s is analogous to the spin-gap phenomenon observed in the underdoped regime of high-T_c cuprates. We also note that the nonmonotonic temperature dependence of the spin susceptibility in a unitarity Fermi gas has also been obtained by the self-consistent T-matrix approximation [56], as well as quantum Monte Carlo simulation [8].

The nonmonotonic temperature dependence of χ_s is obtained over the entire BCS-BEC crossover region, as shown in Fig. 4. Using this, we conveniently introduce the spin-gap temperature T_s as the temperature at which χ_s takes a maximum value. As shown in Fig. 5(a), the spin-gap temperature T_s monotonically increases with increasing the interaction strength. Although T_s is a characteristic temperature without being accompanied by any phase transition, we simply call the temperature region $T_c \leqslant T \leqslant T_s$ the spin-gap regime, where the spin excitations are suppressed.

In Fig. 4, we also plot the experimental result on a ^{6}Li Fermi gas at $(k_Fa_s)^{-1} \simeq -0.8$ (filled circle) [46]. Besides the good agreement of our result with the observed spin susceptibility [55], we find that the experimental result is nearly located at the spin-gap temperature T_s. Thus, when one varies the temperature in this experiment, the decrease of the spin susceptibility is expected, which would be a useful experimental check to confirm the existence of the spin-gap phenomenon.

As shown in Ref. [55], the ETMA also gives a pseudogapped density of states $\rho(\omega)$ in the unitarity limit. In Fig. 6(a), one sees that a dip structure in $\rho(\omega \simeq 0)$ gradually disappears with increasing the temperature from T_c. To see how this pseudogap phenomenon is related to the spin-gap phenomenon in a simple manner, it is helpful to approximately evaluate the spin susceptibility within the neglect of the spin-vertex

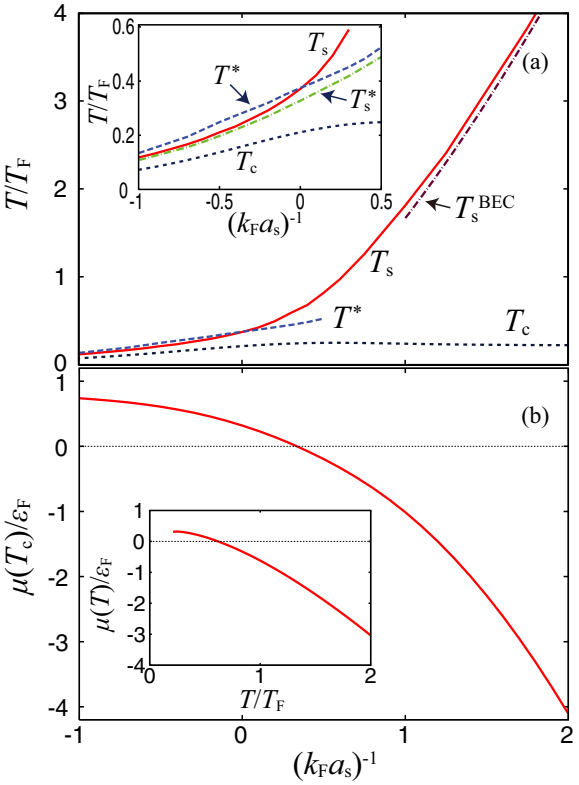

FIG. 5. (Color online) (a) Spin-gap temperature T_s in the BCS-BEC crossover regime of an ultracold Fermi gas. T^* is the pseudogap temperature, which is defined as the temperature at which the density of states $\rho(\omega = 0)$ takes a maximum value. T_s^{BEC} is obtained from Eq. (21). The inset shows the result magnified in the BCS side, where T_s^* is the spin-gap temperature determined from the approximate spin susceptibility $\tilde{\chi}_s$ given by the second line in Eq. (15). (b) Calculated Fermi chemical potential μ at T_c. The inset shows the temperature dependence of μ in the unitarity limit.

correction Λ in Fig. 2, which gives $(\equiv\tilde{\chi}_s)$

$$\tilde{\chi}_s = -T\sum_{\boldsymbol{p},\omega_n} G_{\boldsymbol{p}}^2(i\omega_n)$$
$$= -\sum_{\boldsymbol{p}}\int_{-\infty}^{\infty} dz \int_{-\infty}^{\infty} dz' A_{\boldsymbol{p}}(z)A_{\boldsymbol{p}}(z')\frac{f(z)-f(z')}{z-z'}. \quad (14)$$

Here, $f(z) = [\exp(z/T)+1]^{-1}$ is the Fermi distribution function, and $A_{\boldsymbol{p}}(z) = -\mathrm{Im}[G_{\boldsymbol{p}}(i\omega_n \to z + i\delta)]/\pi$ is the single-particle spectral weight. When the quasiparticle damping described by the imaginary part of the analytic continued self-energy $\mathrm{Im}[\Sigma(\boldsymbol{p}, i\omega_n \to z + i\delta)]$ is weak (which is justified in the weak-coupling regime), the factor $A_{\boldsymbol{p}}(z)A_{\boldsymbol{p}}(z')$ in Eq. (14) becomes large only when $z \simeq z'$. In this case, Eq. (14) is reduced to

$$\tilde{\chi}_s \simeq -\sum_{\boldsymbol{p}}\int_{-\infty}^{\infty} dz A_{\boldsymbol{p}}(z)\frac{df(z)}{dz}\int_{-\infty}^{\infty} dz' A_{\boldsymbol{p}}(z')$$
$$= \int_{-\infty}^{\infty} dz\rho(z)\left(-\frac{df(z)}{dz}\right)$$
$$\simeq \rho(0), \quad (15)$$

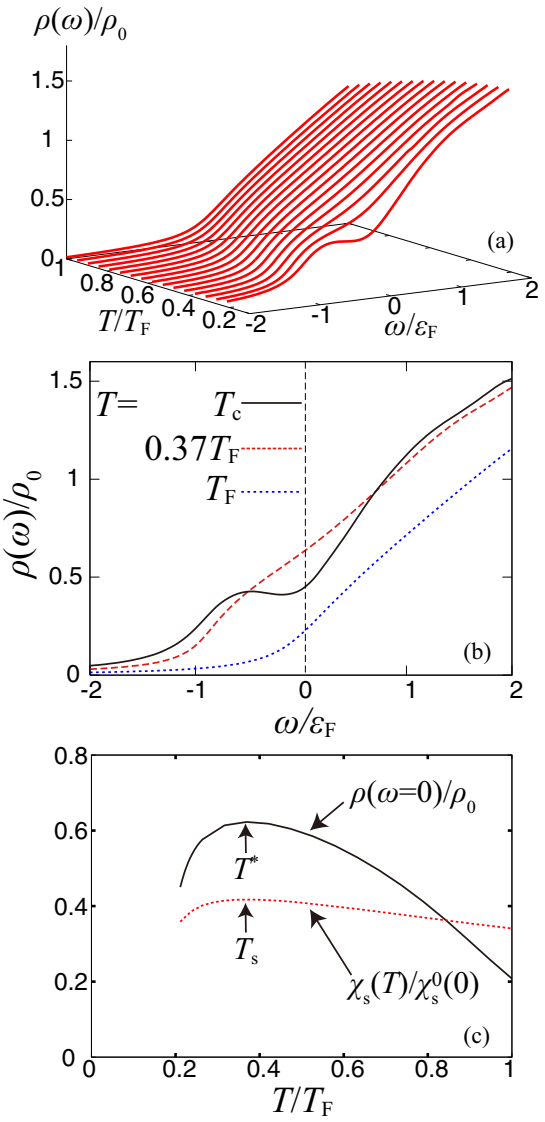

FIG. 6. (Color online) (a) Calculated density of states $\rho(\omega)$ in the unitarity limit. In this panel, the rightmost line shows the result at T_c, where one sees a pseudogap (dip) structure around $\omega = 0$. $\rho_0 = mk_F/(2\pi^2)$ is the density of states at the Fermi level in a free Fermi gas. (b) Density of states $\rho(\omega)$ at some typical temperatures in the unitarity limit. $\rho(\omega = 0)$ takes a maximum value at $T = 0.37T_F$, which we call the pseudogap temperature T^* in this paper. (c) Evaluated $\rho(\omega = 0)$ as a function of temperature in the unitarity limit. For comparison, we also plot χ_s in this panel, where one sees $T_s \simeq T^*$.

where $\rho(z) = \sum_{\boldsymbol{p}} A_{\boldsymbol{p}}(z)$ is just the density of states in Eq. (12). In obtaining the last expression in Eq. (15), we have employed the approximation

$$-\frac{df(z)}{dz} \simeq \delta(z). \tag{16}$$

Equation (15) indicates that the spin-gap behavior of the spin susceptibility directly reflects the temperature dependence of the pseudogapped density of states around $\omega = 0$. Indeed, Fig. 6(b) indicates that $\rho(\omega = 0)$ exhibits nonmonotonic temperature dependence. When we introduce the characteristic temperature T^* at which $\rho(\omega = 0)$ takes a maximum value, Fig. 6(c) shows that $T_s \simeq T^*$, as expected. Since the suppression of $\rho(\omega = 0)$ below T^* is due to the formation of the pseudogap, the spin gap seen in Fig. 3 is found to originate from the pseudogap phenomenon.

We note that the present definition of the pseudogap temperature T^* is a bit different from the ordinary one ($\equiv \tilde{T}^*$) that a dip structure appears in $\rho(\omega \simeq 0)$ below this temperature [1,2]. Since the pseudogap is a crossover phenomenon without being accompanied by any phase transition, the definition of the pseudogap temperature always involves ambiguity to some extent. In this regard, we point out that the coincidence of T_s and T^* shown in Fig. 6(c) indicates that the present definition is convenient in considering the relation between the spin-gap phenomenon and the pseudogap phenomenon. Indeed, the value of the "ordinary" pseudogap temperature equals $\tilde{T}^* = 0.22T_F$ in the unitarity limit, which is only slightly above $T_c = 0.21T_c$ and is much lower than the pseudogap temperature introduced in this paper ($T^* = 0.37T_F$), as well as the spin-gap temperature ($T_s = 0.37T_F$).

We also note that while the low-temperature behavior of $\rho(\omega = 0, T \leqslant T^*)$ in Fig. 4 is due to the pseudogap phenomenon, the high-temperature behavior simply comes from the temperature dependence of the chemical potential μ, which has been already seen in a free Fermi gas. In the noninteracting case, the Fermi chemical potential far below T_F is given by [49]

$$\mu(T) \simeq \varepsilon_F\left[1 - \frac{\pi^2}{12}\left(\frac{T}{T_F}\right)^2\right]. \tag{17}$$

[A similar temperature dependence of μ is also obtained in the unitarity limit, as shown in the inset of Fig. 5(b).] Thus, the density of states $\rho_0(\omega = 0)$ in a free Fermi gas decreases with increasing temperature:

$$\rho_0(\omega = 0) = \frac{m}{2\pi^2}\sqrt{2m\mu(T)} \simeq \frac{mk_F}{2\pi^2}\sqrt{1 - \frac{\pi^2}{12}\left(\frac{T}{T_F}\right)^2}. \tag{18}$$

Figure 7 shows the density of states $\rho(\omega = 0)$ in the BCS-BEC crossover region. Determining T^* from this figure, one finds in Fig. 5(a) that T^* agrees well with the spin-gap temperature T_s, not only in the unitarity limit, but also in the BCS side $(k_F a_s)^{-1} \leqslant 0$. Although T^* is slightly higher than T_s in the BCS regime [see the inset in Fig. 5(a)], it is

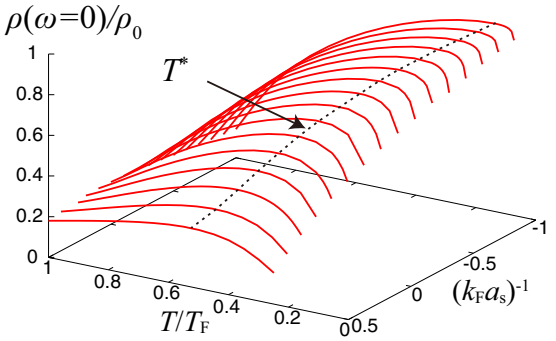

FIG. 7. (Color online) Calculated density of states $\rho(\omega = 0)$ in the BCS-BEC crossover region above T_c. The dotted line shows the pseudogap temperature T^* at which $\rho(0)$ takes a maximum value.

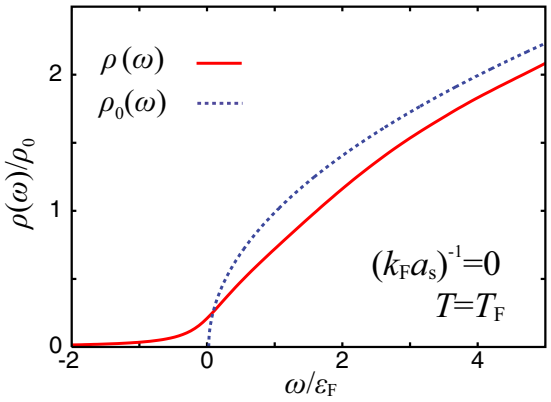

FIG. 8. (Color online) Calculated ETMA density of states $\rho(\omega)$ at T_F in a unitary Fermi gas (solid line). The dashed line shows the density of states $\rho_0(\omega) = (m\sqrt{2m}/2\pi^2)\sqrt{\omega + \mu(T = T_F)}$ in a free Fermi gas.

simply due to the approximation in Eq. (16) in obtaining the last expression in Eq. (15). When we substitute the ETMA density of states into the second line in Eq. (15) and evaluate the spin-gap temperature ($\equiv T_s^*$), T_s^* well reproduces T_s in the BCS side, as shown in the inset in Fig. 5(a). Since there is no experimental technique to directly measure $\rho(\omega)$ in cold Fermi gas physics, our result indicates that the observation of the spin-gap temperature T_s is a useful approach to detect the presence of the pseudogap, at least in the BCS side.

Before ending this section, we briefly explain the reason why $\chi_s(T)$ in Fig. 3 is smaller than the noninteracting result $\chi_s^0(T)$ even far above T_c. When $T \gtrsim T_F$, although pairing fluctuations are weak, particle-particle scatterings still modify the single-particle excitation spectrum, leading to the modification of the density of states $\rho(\omega)$. Indeed, Fig. 8 shows that $\rho(\omega, T = T_F)$ in the unitarity limit is different from the density of states $\rho_0(\omega)$ in the case of a free Fermi gas at the same temperature. Using this modified density of states $\rho(\omega)$ in evaluating the second line in Eq. (15), one obtains $\tilde{\chi}_s < \chi_s^0$ (see Fig. 3). The reason why $\tilde{\chi}_s$ is still larger than the ETMA spin susceptibility χ_s is simply due to the vertex correction Λ ignored in Eq. (15). As pointed out in Ref. [55], when we simply approximate the particle-particle scattering matrix $\Gamma_q(i\nu)$ to the value in the low-energy and low-momentum limit ($\equiv U_{\rm eff}$), the ETMA vertex correction Λ involves the RPA-type Stoner factor [64]. Extending Eq. (15) to include this vertex correction, we obtain

$$\chi_s^{\rm RPA}(T) = \frac{\tilde{\chi}_s(T)}{1 - U_{\rm eff}\tilde{\chi}_s(T)}. \tag{19}$$

Because $U_{\rm eff} < 0$ in the present attractive case ($-U < 0$), the Stoner factor suppresses the spin susceptibility. As shown in Fig. 3, Eq. (19) well describes χ_s in the high-temperature region. Although such agreement is not obtained when $T \lesssim T_F$, this is because vertex corrections beyond the RPA become crucial there due to pairing fluctuations enhanced near T_c.

IV. SPIN-GAP PHENOMENON IN THE BEC REGIME

When $(k_F a_s)^{-1} \gtrsim 0$, T_s gradually deviates from the pseudogap temperature T^*, as seen in Fig. 5(a). In this strong-coupling regime, one cannot ignore the quasiparticle damping effect (which is described by the imaginary part of the analytic continued self-energy) as well as the vertex correction Λ in Fig. 2, so that Eq. (15) is no longer valid.

To understand the physics behind T_s in the BEC regime, we recall that this regime may be viewed as a molecular Bose gas. Since these bound molecules are in the spin-singlet state, they do not contribute to the spin susceptibility. Thus, χ_s in this regime is dominated by Fermi atoms associated with thermal dissociation of molecules. When one approximately treats this situation as a gas mixture of N_M free spinless Bose molecules and N_σ^F free Fermi atoms ($\sigma = \uparrow, \downarrow$), χ_s is evaluated as

$$\chi_s = \lim_{h\to 0} \frac{N_\uparrow^F - N_\downarrow^F}{h}. \tag{20}$$

Using this, one obtains the equation for the spin-gap temperature ($\equiv T_s^{\rm BEC}$) as

$$\frac{1}{\sqrt{2}} \frac{(2\pi m T_s^{\rm BEC})^{\frac{3}{2}}}{(2\pi)^3 N} \exp\left(-\frac{E_b}{T_s^{\rm BEC}}\right) = 4\left[\left(\frac{2E_b + 3T_s^{\rm BEC}}{2E_b - T_s^{\rm BEC}}\right)^2 - 1\right]^{-1}, \tag{21}$$

where $E_b = 1/(ma_s^2)$ is the binding energy of a two-body bound state [42]. [We summarize the derivation of Eq. (21) in the Appendix.] As shown in Fig. 5(a), $T_s^{\rm BEC}$ well describes the spin-gap temperature T_s in the BEC regime. This means that T_s in this regime is dominated by the thermal dissociation of two-body bound molecules.

We point out that Eq. (21) is very similar to the famous Saha equation in classical plasma physics [65],

$$\frac{1}{\sqrt{2}} \frac{(2\pi m T_{\rm Saha})^{\frac{3}{2}}}{(2\pi)^3 N} \exp\left(-\frac{E_I}{T_{\rm Saha}}\right) = \frac{\alpha^2}{1-\alpha}, \tag{22}$$

where E_I is the ionization energy of a particle, which corresponds to the binding energy E_b in Eq. (21). Saha's equation (22) determines the dissociation temperature $T_{\rm Saha}$ at which a given value of the ionization rate α is achieved. The fact of $T_s \simeq T_s^{\rm BEC}$, as well as the similarity between Eqs. (21) and (22), indicate that the spin-gap temperature T_s

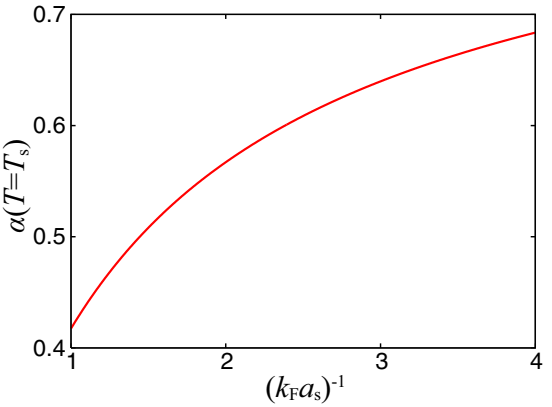

FIG. 9. (Color online) Calculated dissociation rate $\alpha(T = T_s)$ in the BEC regime obtained by equating the right-hand sides of Eqs. (21) and (22).

in the BEC regime is physically similar to Saha's temperature $T_{\rm Saha}$ discussed in classical plasma physics.

Because of the similarity between Eqs. (21) and (22), it is interesting to evaluate the "dissociation rate" $\alpha = [N_\uparrow^{\rm F} + N_\downarrow^{\rm F}]/N$ in the present case. Equating the right-hand sides of these equations, we find that $\alpha(T_{\rm s}) \simeq 0.5$ when $(k_{\rm F}a_{\rm s})^{-1} \sim 1.5$, as shown in Fig. 9. This means that around this interaction strength, bound molecules are thermally dissociated into Fermi atoms at $T \sim T_{\rm s}$. We briefly note that $\alpha(T_{\rm s})$ approaches unity in the extreme BEC limit $[(k_{\rm F}a_{\rm s})^{-1} \to \infty]$.

V. SUMMARY

To summarize, we have discussed spin-gap phenomena in the normal state of an ultracold Fermi gas. Including strong pairing fluctuations within the framework of an extended T-matrix approximation, we have calculated the uniform spin susceptibility $\chi_{\rm s}$ in the BCS-BEC crossover region. We showed that $\chi_{\rm s}$ exhibits nonmonotonic temperature dependence. In particular, $\chi_{\rm s}$ is anomalously suppressed near $T_{\rm c}$, which is similar to the spin-gap phenomenon known in high-$T_{\rm c}$ cuprates. To characterize the spin-gap phenomenon in the present case, we have introduced the spin-gap temperature $T_{\rm s}$ as the temperature at which $\chi_{\rm s}$ takes a maximum value. Determining $T_{\rm s}$ over the entire BCS-BEC crossover region, we have identified the spin-gap regime, which is wider for a stronger pairing interaction, as expected.

We clarified how the spin-gap phenomenon is related to the pseudogap phenomenon appearing in the single-particle density of states $\rho(\omega)$. Introducing the pseudogap temperature T^* as the temperature at which $\rho(\omega = 0)$ takes a maximum value, we found that T^* agrees well with $T_{\rm s}$, when $(k_{\rm F}a_{\rm s})^{-1} \lesssim 0$. Since the suppression of $\rho(\omega \simeq 0)$ below T^* is characteristic of the pseudogap phenomenon, this agreement means that the spin-gap phenomenon in the BCS side originates from the pseudogapped density of states.

The spin-gap temperature $T_{\rm s}$ gradually deviates from T^* as one enters the BEC side $[(k_{\rm F}a_{\rm s})^{-1} \gtrsim 0]$. In this strong-coupling regime, the system may be viewed as a gas mixture of tightly bound molecules and unpaired Fermi atoms. Since the former molecules are in the spin-singlet state, only the latter fermions contribute to the spin susceptibility. Indeed, we showed that $T_{\rm s}$ in the BEC regime is well described by the spin-gap temperature $T_{\rm s}^{\rm BEC}$, which is evaluated in a model gas mixture of two-component free fermions and free spinless bosons. We also showed that the equation for $T_{\rm s}^{\rm BEC}$ is similar to Saha's equation in classical plasma physics. The good agreement of $T_{\rm s}$ with $T_{\rm s}^{\rm BEC}$, as well as the similarity between the equation for $T_{\rm s}^{\rm BEC}$ and Saha's equation, indicate that the spin-gap phenomenon in the BEC regime is dominated by thermal dissociation of tightly bound molecules. Evaluating the dissociation rate $\alpha(T = T_{\rm s})$, we obtain $\alpha(T_{\rm s}) \sim 0.5$ when $(k_{\rm F}a_{\rm s})^{-1} \sim 1.5$.

In cold Fermi gas physics, although it is a crucial problem whether the pseudogap really exists or not, there is no experimental technique to directly measure the single-particle density of states, which makes the pseudogap problem difficult. Since the uniform spin susceptibility $\chi_{\rm s}$ is observable in ultracold Fermi gases, our result would be useful for the detection of the pseudogap phenomenon through this quantity in this system.

The pseudogap and the spin-gap phenomena are considered as crucial keys to clarify the pairing mechanism of high-$T_{\rm c}$ cuprates. Among various ideas proposed to explain these anomalous phenomena, the preformed-pair scenario is a strong candidate. In this regard, although there exist various differences between high-$T_{\rm c}$ cuprates and cold Fermi gases, such as the pairing symmetry (d-wave state and s-wave state), dimensionality, and the presence of a crystal lattice, an ultracold Fermi gas is still a useful system to assess this scenario in a quantitative manner, because this system is dominated simply by pairing fluctuations. That is, if the pseudogap and the spin gap are not remarkable even in a two-dimensional ultracold Fermi gas compared with the case of high-$T_{\rm c}$ cuprates, it means that pairing fluctuations are not enough to fully produce the pseudogap and spin-gap phenomena in high-$T_{\rm c}$ cuprates. If these phenomena are much more remarkable in an ultracold Fermi gas than in high-$T_{\rm c}$ cuprates, the preformed-pair scenario is a promising idea in high-$T_{\rm c}$ cuprates, although this mechanism is considered to be suppressed to some extent there. In addition, the BCS-BEC crossover physics has clarified that $T_{\rm c}$ is lowered by pairing fluctuations compared with the mean field $T_{\rm c}$ (where pairing fluctuations are completely ignored). This implies that if one can approach the superfluid instability by suppressing the effect of pairing fluctuations, one might be able to raise $T_{\rm c}$ without increasing the interaction strength. Since obtaining higher $T_{\rm c}$ is always an exciting challenge in condensed matter physics, the cold Fermi gas system is expected to be convenient to systematically examine whether or not we can manipulate the suppression effect of pairing fluctuations on $T_{\rm c}$ without tuning the interaction strength. In this regard, the pseudogap and spin gap would be useful phenomena to detect the strength of pairing fluctuations when they can be tuned. Thus, our results would also contribute to further development of the field of high-$T_{\rm c}$ superconductivity, in addition to cold Fermi gas physics.

ACKNOWLEDGMENTS

We would like to thank D. Inotani for useful discussions. Y.O. was supported by a Grant-in-Aid for Scientific Research from MEXT in Japan (Grants No. 25400418, No. 25105511, and No. 23500056).

APPENDIX: DERIVATION OF EQ. (21)

In the classical regime ($T \gg T_{\rm F}$), $N_\sigma^{\rm F}$ and $N_{\rm M}$ are given by, respectively,

$$N_\sigma^{\rm F} = \sum_{\boldsymbol{p}} \exp\left(-\frac{\varepsilon_{\boldsymbol{p}} - \mu - \sigma h/2}{T}\right) = \frac{3\sqrt{\pi}N}{8}\left(\frac{T}{\varepsilon_{\rm F}}\right)^{3/2} \lambda \exp\left(\frac{\sigma h}{2T}\right), \tag{A1}$$

$$N_{\rm M} = \sum_{\boldsymbol{q}} \exp\left(-\frac{\varepsilon_{\boldsymbol{q}}/2 - 2\mu - E_{\rm b}}{T}\right) = \frac{3\sqrt{2\pi}N}{4}\left(\frac{T}{\varepsilon_{\rm F}}\right)^{3/2} \lambda^2 \exp\left(\frac{E_{\rm b}}{T}\right). \tag{A2}$$

Here, $E_b = 1/(ma_s^2)$ is the binding energy of a molecule, and $\lambda = \exp(\mu/T)$ is the fugacity. By substituting Eqs. (A1) and (A2) into the number equation, $N = N_\uparrow^F + N_\downarrow^F + 2N_M$, one obtains

$$\lambda = \frac{1}{4\sqrt{2}} \exp\left(-\frac{E_b}{T}\right) \times \left[\sqrt{1 + \frac{32}{3}\sqrt{\frac{2}{\pi}}\left(\frac{T}{\varepsilon_F}\right)^{-3/2} \exp\left(\frac{E_b}{T}\right)} - 1\right]. \quad \text{(A3)}$$

Evaluating Eq. (20) using Eq. (A1), we obtain

$$\chi_s = \frac{\sqrt{\pi}}{2}\sqrt{\frac{T}{\varepsilon_F}}\lambda\chi_s^0(0), \quad \text{(A4)}$$

where $\chi_s^0(0)$ is the spin susceptibility in a free Fermi gas at $T = 0$. The spin-gap temperature T_s^{BEC} is determined from the condition $\partial\chi_s/\partial T = 0$, which gives

$$\sqrt{\frac{\varepsilon_F}{T}}\lambda + 2\sqrt{\varepsilon_F T}\frac{\partial\lambda}{\partial T} = 0. \quad \text{(A5)}$$

In Eq. (A5), the derivative of λ in terms of T is given by

$$\frac{\partial\lambda}{\partial T} = \frac{3\lambda}{2T}\frac{\left(\frac{4\sqrt{2}}{3}\frac{E_b}{T} - 2\sqrt{2}\right)\lambda\exp\left(\frac{E_b}{T}\right) - 1}{4\sqrt{2}\lambda\exp\left(\frac{E_b}{T}\right) + 1}. \quad \text{(A6)}$$

By substituting Eqs. (A3) and (A6) into Eq. (A5), we obtain Eq. (21).

We briefly note that the Saha equation (22) is obtained when one divides $\alpha^2 = [N_\uparrow^F + N_\downarrow^F]^2/N^2$ by $2N_M/N^{\sim}(= 1 - \alpha)$ with $h = 0$.

[1] S. Tsuchiya, R. Watanabe, and Y. Ohashi, Phys. Rev. A **80**, 033613 (2009); **82**, 033629 (2010); **84**, 043647 (2011).
[2] R. Watanabe, S. Tsuchiya, and Y. Ohashi, Phys. Rev. A **86**, 063603 (2012); **88**, 013637 (2013).
[3] Q. J. Chen and K. Levin, Phys. Rev. Lett. **102**, 190402 (2009).
[4] H. Hu, X.-J. Liu, P. D. Drummond, and H. Dong, Phys. Rev. Lett. **104**, 240407 (2010).
[5] E. J. Mueller, Phys. Rev. A **83**, 053623 (2011).
[6] P. Magierski, G. Wlazlowski, and A. Bulgac, Phys. Rev. Lett. **107**, 145304 (2011).
[7] S-Q. Su, D. E. Sheehy, J. Moreno, and M. Jarrell, Phys. Rev. A **81**, 051604(R) (2010).
[8] G. Wlazłowski P. Magierski, J. E. Drut, A. Bulgac, and K. J. Roche, Phys. Rev. Lett. **110**, 090401 (2013).
[9] J. T. Stewart, J. P. Gaebler, and D. S. Jin, Nature (London) **454**, 744 (2008).
[10] J. P. Gaebler, J. T. Stewart, T. E. Drake, D. S. Jin, A. Perali, P. Pieri, and G. C. Strinati, Nat. Phys. **6**, 569 (2010).
[11] A. Perali, F. Palestini, P. Pieri, G. C. Strinati, J. T. Stewart, J. P. Gaebler, T. E. Drake, and D. S. Jin, Phys. Rev. Lett. **106**, 060402 (2011).
[12] M. Feld, B. Fröhlich, E. Vogt, M. Koschorreck, and M. Köhl, Nature (London) **480**, 75 (2011).
[13] S. Nascimbène, N. Navon, K. J. Jiang, F. Chevy, and C. Salomon, Nature (London) **463**, 1057 (2010).
[14] S. Nascimbène, N. Navon, S. Pilati, F. Chevy, S. Giorgini, A. Georges, and C. Salomon, Phys. Rev. Lett. **106**, 215303 (2011).
[15] N. Navon, S. Nascimbène, F. Chevy, and C. Salomon, Science **328**, 729 (2010).
[16] Ch. Renner, B. Revaz, J.-Y. Genoud, K. Kadowaki, and Ø. Fischer, Phys. Rev. Lett. **80**, 149 (1998).
[17] For reviews, see, A. Damascelli, Z. Hussain, and Z.-X. Shen, Rev. Mod. Phys. **75**, 473 (2003); P. Lee, N. Nagaosa, and X. Wen, *ibid*. **78**, 17 (2006).
[18] Ø. Fischer, M. Kugler, I. Maggio-Aprile, and C. Berthod, Rev. Mod. Phys. **79**, 353 (2007).
[19] Y. Yanase and K. Yamada, J. Phys. Soc. Jpn. **70**, 1659 (2001).
[20] D. Pines, Z. Phys. B **103**, 129 (1996).
[21] A. Kampf and J. R. Schrieffer, Phys. Rev. B **41**, 6399 (1990).
[22] S. Chakravarty, R. B. Laughlin, D. K. Morr, and C. Nayak, Phys. Rev. B **63**, 094503 (2001).
[23] B. Fauqué, Y. Sidis, V. Hinkov, S. Pailhès, C. T. Lin, X. Chaud, and P. Bourges, Phys. Rev. Lett. **96**, 197001 (2006).
[24] S. A. Kivelson, I. P. Bindloss, E. Fradkin, V. Oganesyan, J. M. Tranquada, A. Kapitulnik, and C. Howald, Rev. Mod. Phys. **75**, 1201 (2003).
[25] T. Wu, H. Mayaffre, S. Krämer, M. Horvatić, C. Berthier, W. N. Hardy, R. Liang, D. A. Bonn, and M.-H. Julien, Nature (London) **477**, 191 (2011).
[26] R. Daou, J. Chang, D. LeBoeuf, O. Cyr-Choinière, F. Laliberté, N. Doiron-Leyraud, B. J. Ramshaw, R. Liang, D. A. Bonn, W. N. Hardy, and L. Taillefer, Nature (London) **463**, 519 (2010).
[27] J.-H. Ma, Z.-H. Pan, F. C. Niestemski, M. Neupane, Y.-M. Xu, P. Richard, K. Nakayama, T. Sato, T. Takahashi, H.-Q. Luo, L. Fang, H.-H. Wen, Z. Wang, H. Ding, and V. Madhavan, Phys. Rev. Lett. **101**, 207002 (2008).
[28] M. Hashimoto, R.-H. He, K. Tanaka, J.-P. Testaud, W. Meevasana, R. G. Moore, D. Lu, H. Yao, Y. Yoshida, H. Eisaki, T. P. Deveraux, Z. Hussain, and Z.-X. Shen, Nat. Phys. **6**, 414 (2010).
[29] W. Zhang, C. L. Smallwood, C. Jozwiak, T. L. Miller, Y. Yoshida, H. Eisaki, D.-H. Lee, and A. Lanzara, Phys. Rev. B **88**, 245132 (2013).
[30] E. Timmermans, K. Furuya, P. W. Milonni, and A. K. Kerman, Phys. Lett. A **285**, 228 (2001).
[31] S. Giorgini, L. P. Pitaevskii, and S. Stringari, Rev. Mod. Phys. **80**, 1215 (2008).
[32] C. Chin, R. Grimm, P. Julienne, and E. Tiesinga, Rev. Mod. Phys. **82**, 1225 (2010).
[33] I. Bloch, J. Dalibard, and W. Zwerger, Rev. Mod. Phys. **80**, 885 (2008).
[34] V. Gurarie and L. Radihovsky, Ann. Phys. **322**, 2 (2007).
[35] C. A. Regal, M. Greiner, and D. S. Jin, Phys. Rev. Lett. **92**, 040403 (2004).
[36] M. W. Zwierlein, C. A. Stan, C. H. Schunck, S. M. F. Raupach, A. J. Kerman, and W. Ketterle, Phys. Rev. Lett. **92**, 120403 (2004).

[37] J. Kinast, S. L. Hemmer, M. E. Gehm, A. Turlapov, and J. E. Thomas, Phys. Rev. Lett. **92**, 150402 (2004).
[38] M. Bartenstein, A. Altmeyer, S. Riedl, S. Jochim, C. Chin, J. H. Denschlag, and R. Grimm, Phys. Rev. Lett. **92**, 203201 (2004).
[39] D. M. Eagles, Phys. Rev. **186**, 456 (1969).
[40] A. J. Leggett, in *Modern Trends in the Theory of Condensed Matter*, edited by A. Pekalski and J. Przystawa (Springer Verlag, Berlin, 1980), p. 14.
[41] P. Nozières and S. Schmitt-Rink, J. Low Temp. Phys. **59**, 195 (1985).
[42] C. A. R. Sa de Melo, M. Randeria, and J. R. Engelbrecht, Phys. Rev. Lett. **71**, 3202 (1993).
[43] Y. Ohashi and A. Griffin, Phys. Rev. Lett. **89**, 130402 (2002).
[44] A. Perali, P. Pieri, G. C. Strinati, and C. Castellani, Phys. Rev. B **66**, 024510 (2002).
[45] A. A. Abrikosov, L. P. Gorkov, and I. E. Dzyaloshinski, *Methods of Quantum Field Theory in Statistical Mechanics* (Dover, New York, 1963), Chap. 4.
[46] C. Sanner, E. J. Su, A. Keshet, W. Huang, J. Gillen, R. Gommers, and W. Ketterle, Phys. Rev. Lett. **106**, 010402 (2011).
[47] A. Sommer, M. Ku, G. Roati, and M. W. Zwierlein, Nature (London) **472**, 201 (2011).
[48] Y.-R. Lee, T. T. Wang, T. M. Rvachov, J.-H. Choi, W. Ketterle, and M.-S. Heo, Phys. Rev. A **87**, 043629 (2013).
[49] See, for example, R. Kubo, *Statistical Mechanics* (North-Holland, Amsterdam, 1988), Chap. 4.
[50] Y. Yoshinari, H. Yasuoka, Y. Ueda, K. Koga, and K. Kosuge, J. Phys. Soc. Jpn. **59**, 3698 (1990).
[51] M. Randeria, N. Trivedi, A. Moreo, and R. T. Scalettar, Phys. Rev. Lett. **69**, 2001 (1992).
[52] N. Trivedi and M. Randeria, Phys. Rev. Lett. **75**, 312 (1995).
[53] X.-J. Liu and H. Hu, Europhys. Lett. **75**, 364 (2006).
[54] M. M. Parish, F. M. Marchetti, A. Lamacraft, and B. D. Simons, Nat. Phys. **3**, 124 (2007).
[55] T. Kashimura, R. Watanabe, and Y. Ohashi, Phys. Rev. A **86**, 043622 (2012).
[56] T. Enss and R. Haussmann, Phys. Rev. Lett. **109**, 195303 (2012).
[57] E. Taylor, S. Zhang, W. Schneider, and M. Randeria, Phys. Rev. A **84**, 063622 (2011).
[58] F. Palestini, P. Pieri, and G. C. Strinati, Phys. Rev. Lett. **108**, 080401 (2012).
[59] In our numerical calculations, we take $\omega_c = 10^4 \varepsilon_F$ (where ε_F is the Fermi energy). We have confirmed that our results do not depend on the value of ω_c when $\omega_c \gtrsim O(10^4 \varepsilon_F)$.
[60] We have numerically confirmed that the "magnetization" $N_\uparrow - N_\downarrow$ is proportional to h, when $h/\varepsilon_F = O(10^{-2})$.
[61] P. Nozières, *Theory of Interacting Fermi Systems* (Benjamin, New York, 1964), Chap. 6.
[62] In the dressed Green's function $G_{\boldsymbol{p},\sigma}(i\omega_n)$ in Eq. (3), we note that the effective magnetic field h is involved in both the bare Green's function $G^0_{\boldsymbol{p},\sigma}(i\omega_n)$ and the self-energy $\Sigma_{\boldsymbol{p},\sigma}(i\omega_n)$. When we take into account only h in the former part in carrying out the h derivative in Eq. (8), the resulting spin susceptibility is diagrammatically given by Fig. 2(a), where the spin-vertex correction (triangle) is replaced by the bare vertex (solid circle). This treatment is clearly incomplete in the sense that all h's involved in the dressed Green's function $G_{\boldsymbol{p},\sigma}(i\omega_n)$ are not equally taken into account. Indeed, the Ward identity in Eq. (11) is not satisfied in this case. In this sense, satisfying the Ward identity in the present case is the same in that we treat all h's equally in the dressed Green's function in calculating the spin susceptibility.
[63] D. J. Thouless, Ann. Phys. **10**, 553 (1960).
[64] K. Yosida, *Theory of Magnetism* (Springer-Verlag, Berlin, 1996), Chap. 14.
[65] M. Saha, Proc. R. Soc. A **99**, 135 (1921).